Chapter 8

Detection of Nitric Oxide by Electron Paramagnetic Resonance Spectroscopy: Spin-Trapping with Iron-Dithiocarbamates

Luisa B. Maia and José J.G. Moura

Abstract

Electron paramagnetic resonance (EPR) spectroscopy is the ideal methodology to identify radicals (detection and characterization of molecular structure) and to study their kinetics, in both simple and complex biological systems. The very low concentration and short life-time of NO and of many other radicals do not favor its direct detection and spin-traps are needed to produce a new and persistent radical that can be subsequently detected by EPR spectroscopy.

In this chapter, we present the basic concepts of EPR spectroscopy and of some spin-trapping methodologies to study NO. The "strengths and weaknesses" of iron-dithiocarbamates utilization, the NO traps of choice for the authors, are thoroughly discussed and a detailed description of the method to quantify the NO formation by molybdoenzymes is provided.

Key words Nitric oxide radical, Electron paramagnetic resonance (EPR), Spin-trap, Iron-dithiocarbamate, Nitrite, Xanthine oxidoreductase, Aldehyde oxidoreductase

Abbreviations

AOR	Aldehyde oxidoreductase
CPTIO	2-(4-Carboxyphenyl)-4,4,5,5-tetramethyl-imidazoline-1-oxyl-3-oxide
DETC	Diethyldithiocarbamate
DMPO	5,5-Dimethyl-1-pyrroline *N*-oxide
EPR	Electron paramagnetic resonance
Fe-$(TC)_2$	Iron-*bis*-dithiocarbamates
Fe^{2+}-$(TC)_2$	Ferrous-*bis*-dithiocarbamate
Fe^{3+}-$(TC)_2$	Ferric-*bis*-dithiocarbamate
Hb	Hemoglobin
MGD	*N*-methyl-D-glucamine-dithiocarbamate
MNIC	Mononitrosyl-iron complex
MNP	2-Methyl-2-nitrosopropane
NO	Nitric oxide radical (•NO)

Kapuganti Jagadis Gupta (ed.), *Plant Nitric Oxide: Methods and Protocols*, Methods in Molecular Biology, vol. 1424,
DOI 10.1007/978-1-4939-3600-7_8,

ST Spin-trap molecule
TEMPO 2,2,6,6-Tetramethylpiperidinyl-*N*-oxyl
XO Xanthine oxidase

1 Introduction

Nitric oxide radical (chemical formula •NO, abbreviated as NO), is a signaling molecule involved in several physiological processes, in mammals, plants, and prokaryotes [1–8]. However, while in some situations the participation of NO is already compelling, in many other cases its involvement is less certain. Also the sources of NO are a matter of debate. Presently, different pathways are thought to contribute to the NO generation, including mammalian and prokaryotic NO synthases and several mammalian, plant, and prokaryotic "non-dedicated" nitrite reductases, that make use of metalloproteins, present in cells to carry out other functions, to reduce nitrite to NO. Hence, the advancement of knowledge of NO Biology demands for methods, not only to quantify, but also to unequivocally identify the NO. Several methodologies were developed to measure NO, either indirectly, quantifying for example the NO oxidation products, and directly, exploring different properties of NO, such as its ability to react with ozone to produce light (chemiluminescence) or its radical nature (electron paramagnetic resonance (EPR) spectroscopy).

NO, with its 11 valence electrons, has an unpaired electron in a π-antibonding orbital, polarized toward the nitrogen atom (the unpaired electron is delocalized over the nitrogen) (Fig. 1). As a result, NO is a radical molecule and this feature makes the EPR spectroscopy an ideal methodology to both quantify and identify NO.

1.1 Basic EPR Theory

Because of its spin, the electron has a magnetic moment and, in the presence of an applied magnetic field (B_0), the magnetic moment has two allowed orientations (the principles of quantum mechanics states that only two energy states or levels are allowed), corresponding to two spin states, with energies (E),

$$E_\alpha = +\tfrac{1}{2} g \mu_B B_0 \quad \text{and} \quad E_\beta = -\tfrac{1}{2} g \mu_B B_0 \qquad (1)$$

where μ_B is the Bohr magneton (=9.2740154 (31) × 10^{-24} JT^{-1}) and the parameter g (also called g-factor) is a constant that is dependent on the nature, structure, and environment of the paramagnetic species (for a free electron, g = 2.0023). Transitions between the two states can be induced when electromagnetic radiation with energy equal to $\Delta E = E_\alpha - E_\beta$ is applied perpendicularly to the external magnetic field, or better saying, radiation of appropriate frequency, υ (because $E = h\upsilon$, where h is the Planck constant (=6.6260755 (40) × 10^{-34} Js)),

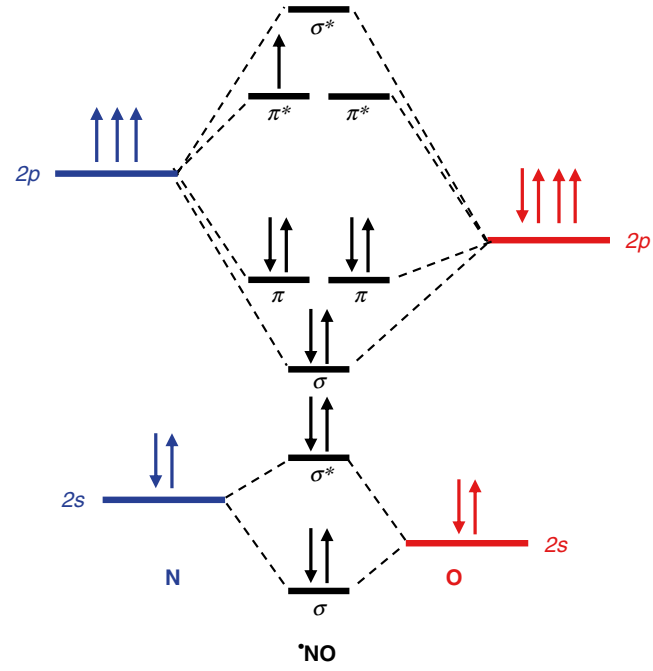

Fig. 1 Molecular orbital diagram for NO

$$h\upsilon = \Delta E = g\mu_B B_0 \tag{2a}$$

This is the relationship (the resonance condition) that must be satisfied for microwave radiation ($\approx 10^9$–10^{11} Hz) absorption to occur. Hence, in simple words, in EPR spectroscopy one detects unpaired electrons by measuring the absorption of electromagnetic radiation, when the paramagnetic sample is placed in a magnetic field (e.g., $B_0 \approx 10$–600 mT for a spectrometer that operates at ≈9.5 GHz). One can also quantify the concentration of the paramagnetic species, by simple calculation of the area under the absorption line (that is, the double integral of the spectrum, because the EPR spectrum is recorded as the first derivative of absorption). Contrary to absorbance measurements, the intensity of an EPR spectrum is independent of the species that has originated it and, thus, quantification does not require the previous knowledge of an extinction coefficient.

The parameter g, which can be identified as the spectroscopic manifestation of the magnetic moment, is obtained experimentally from Eq. 2a,

$$g = (h / \mu_B)(\upsilon / B_0) = 7.14 \times 10^{-11}\,\mathrm{Ts}\,(\upsilon(\mathrm{s}^{-1}) / B_0(\mathrm{T})) \tag{2b}$$

It is a measure of the local magnetic and electric fields experienced by the unpaired electron(s) and it provides valuable information regarding the nature, structure, and environment of the paramagnetic species and, therefore, information about the identity of the paramagnetic species. Regarding nature of radical species, while

paramagnetic transition metal ions, such as Mo^{5+}, Fe^{3+}, or Cu^{2+} (with d^1, d^5, or d^9 configuration, respectively), display a large range of g values ($g \approx 0$–10), organic radicals have g values around the one of free electron ($g \approx 2$). Nevertheless, the presence of electron donor or acceptor groups modify the g value (e.g., the delocalization of the unpaired electron over heteroatoms generally causes an increase in the g value) and such effects can be used as "diagnostic" of the structure of the detectable paramagnetic species. A substantial understanding of the EPR phenomenon is required to obtain structural information from this technique (which is outside the scope of this chapter, please refer to refs. 9–11). More simple and relevant in the context of this chapter, is the effect caused by the presence of neighboring nuclei with nuclear magnetic moment ($I \neq 0$, e.g., $I(^1H) = 1/2$, $I(^{14}N) = 1$, or $I(^{15}N) = 1/2$), which create a local magnetic field that is superimposed onto the applied one (B_0). In general, there will be $2I+1$ orientations for a given nuclear spin ($2I+1$ allowed energy states); the unpaired electron experiences these different magnetic fields and the EPR signal is split into $2I+1$ lines of equal intensity and equally spaced. For example, for one unpaired electron localized into a nitrogen atom ($I(^{14}N) = 1$), the EPR signal consists of a 1:1:1 triplet of equally spaced lines. The magnitude of the splitting between the lines is called hyperfine splitting constant (if it arises from the "parent" nucleus) or superhyperfine splitting constant (when it arises from a satellite nucleus; both abbreviated as a); equivalent nuclei give rise to equivalent splitting constant values, while nonequivalent nuclei originate different patterns of lines. In addition, the EPR spectrum reflects also the environment of the paramagnetic species (physical state, solvent) which also determine its "motion" (refer to refs. 9–11).

In summary, EPR is a powerful spectroscopy that probes the paramagnetic center, by defining the size and shape of the magnetic moment produced by the unpaired electron(s) and by characterizing the magnetic field created by the vicinity of the unpaired electron(s). It can demonstrate the presence of paramagnetic species (radicals and some transition metal ions) and provide information on its concentration, nature and structure (identity) mobility, and intra- and intermolecular interactions. Moreover, as only unpaired electrons are able to absorb microwave radiation under these conditions, the EPR spectroscopy is specific for paramagnetic species. Hence, regardless of the complexity of the sample, there will be no spectroscopic signal (absorption) apart from the one of the paramagnetic species (i.e., there will be no background signal from the biological matrix).

1.2 Spin-Trapping

In spite of its radical nature, the characteristics of NO (and of many other radicals) do not favor its direct detection by EPR spectroscopy [7, 12–17]: (1) generation in low concentration (e.g., 10^{-9}–10^{-7} M in humans), (2) ability to freely permeate membranes (k diffusion $\approx 10^{10}$–10^{11} M^{-1} s^{-1}), (3) reactivity with dioxygen ($k \approx 10^6$–10^7

$M^{-2}s^{-1}$), (4) high reactivity with superoxide anion radical ($k \approx 10^9$–10^{10} $M^{-1}s^{-1}$), (5) with metalloproteins (mostly haems and labile [4Fe–4S] centers, to yield nitrosyl derivates (metal-N=O)), and (6) with cysteine residues and other thiols (to yield *S*-nitrosothiol derivates (–S–N=O)). Hence, the NO available to be detected (difference between NO formed and NO consumed) is usually rather low, particularly in complex biological samples, where several "sinks" of NO could be present.

As a result, with the exception of a few radicals with long half-life (e.g., ascorbyl and tocopheroxyl radicals that are intrinsically stabilized by electron delocalization and less reactive), one needs first to "stabilize" the radical to, then, be able to detect it. This "stabilization" is achieved by spin-trapping and it involves the reaction of the radical ($X^{\bullet}$) with a spin-trap molecule (ST) to yield a new and persistent radical ($^{\bullet}$ST-X; Eq. 3) that can be subsequently detected by EPR spectroscopy.

$$X^{\bullet} + ST \rightarrow {}^{\bullet}ST\text{-}X \qquad (3)$$

In practical terms, the spin trap, in many cases a nitrone (R_1-(R_2=)N^+–O^-, e.g., DMPO) or a nitroso (R_1-N=O, e.g., MNP) compound, is added at an appropriate concentration to ensure the effective trapping of the radicals present in the sample (the trap concentration is dictated by the ratio between the rate constant of $^{\bullet}$ST-X formation and the rate constants of radical consumption reactions; the slower the $^{\bullet}$ST-X formation reaction, the higher the trap concentration should be, in order to be able to effectively compete with the other radical consumption reactions). The stable nitroxide radicals formed (R_1-(X-R_2-) N–$O^{\bullet}$ or R_1-N(-X)–$O^{\bullet}$) are, then, detected. Because different $^{\bullet}$ST-X radicals give rise to distinctive EPR signals (determined by the $X^{\bullet}$ structure), the spectra can be used to identify the radical $X^{\bullet}$, as well as, to follow the kinetics of its formation/consumption. This approach has been widely used to study not only the obvious *small* radicals, such as the superoxide anion ($O_2^{\bullet -}$) and hydroxyl ($HO^{\bullet}$) radicals [18–22], but also radicals on biomacromolecules, proteins, lipids, and nucleic acids [23–25].

To trap NO, three main types of spin-traps have been explored, nitronyl nitroxides, hemoglobin (and myoglobin), and iron-*bis*-dithiocarbamates.

Nitronyl nitroxides (e.g., CPTIO) are *N*-oxo-imidazoles radicals that react with NO to yield nitrogen dioxide radical ($^{\bullet}NO_2$) and an imino-nitroxide radical [26, 27]. Hence, there is no NO trapping, what hampers studies with labeled nitrogen (see below how convenient this could be). In addition, because both the spin-trap itself and its product (the imino-nitroxide radical) are radicals, the resulting EPR spectrum obtained after the reaction of NO with the nitronyl nitroxide is the sum of two overlapped signals, what makes the spectrum interpretation and quantification not a straightforward task [28]. Moreover, also because these spin-traps give rise to an EPR signal, one cannot increase their concentration

to overcome the relatively low rate constant of the reaction of nitronyl nitroxide with NO ($k \approx 10^3$ $M^{-1}s^{-1}$). On the other hand, the nitrogen dioxide radical formed reacts with NO to convert it into nitrite [8, 29, 30] and, thus, leads to an undervaluation of NO concentration (in other words, the ratio between the NO and the imino-nitroxide signal is not one to one) [28]. The nitrogen dioxide radical could also compromise the integrity of the biological sample (it is a powerfully oxidizing and nitrating agent that can nitrate protein residues, fatty acids, and nucleotides) [8]. Finally, because nitroxides are good oxidants, one must evaluate if these compounds are interfering with redox chemistry of the system under study [31, 32].

Hemoglobin (Hb) (and also myoglobin) has been widely used in NO research. It is cheap, reacts with NO with high rate constants [$k > 10^7$ $M^{-1}s^{-1}$ (*reviewed in* ref. 8)] and can be used in UV–visible [33] and EPR spectroscopy. Besides being used in detection/quantification, the ability of hemoglobin to trap NO has also been used to "remove" NO from a system or to confirm its presence (in a negative control assay). Both oxy-hemoglobin ($(Hb)Fe^{2+}–O_2$; Eq. 4) and deoxy-hemoglobin ($(Hb)Fe^{2+}$; Eq. 5) react with NO (*reviewed in ref.* 8):

$$(Hb)Fe^{2+} \quad O_2 + {}^{\bullet}NO \rightarrow (Hb)Fe^{3+} + NO_3^- \tag{4}$$

$$(Hb)Fe^{2+} + {}^{\bullet}NO \rightarrow (Hb)Fe^{2+} \quad NO \tag{5}$$

Met-hemoglobin ($(Hb)Fe^{3+}$; Eq. 4), with its oxidized iron atom (Fe^{3+}, d^5 configuration), can be easily followed by EPR spectroscopy, with high sensitivity at low (liquid helium) temperatures (≈100 nM, although the use of liquid helium increases the assays cost) [34]. However, there is no NO trapping and the formation of methemoglobin is not specific for NO, as peroxynitrite and other oxidants can also oxidize hemoglobin. Alternatively, one can follow the formation of the stable hemoglobin–NO complex ($(Hb)Fe^{2+}–NO$, $K_d \approx 10^{-12}$ to 10^{-10} M [8]; Eq. 5), at 77 K (liquid nitrogen temperature), without compromising the sensitivity (≈200 nM) [34]. The assay has to be carried out under anaerobic conditions (to maintain the deoxygenation of hemoglobin) and the EPR signal is more complex in this case, but can be deconvoluted (by simulation) in three main species, penta- and hexacoordinated α-Hb-NO and hexacoordinated β-Hb-NO [34–38]. Furthermore, since NO is effectively trapped by hemoglobin, experiments with isotopically labeled nitrogen (^{15}N) can be carried out to undoubtedly identify the NO source (this is due to the fact that naturally abundant isotope of nitrogen (^{14}N) and ^{15}N have different nuclear magnetic moments (1 and 1/2) and thus originate different splittings).

The last type of spin-traps here described, and the one whose utilization is detailed discussed, makes use of the high affinity of NO to bind to ferrous chelates to detect it: iron- *bis* -dithiocarbamates

($Fe\text{-}(TC)_2$) [39–45]. A dithiocarbamate (Fig. 2b) is a derivate of the carbamic acid (Fig. 2a), in which both oxygen atoms were replaced by sulfur—key to coordinate the iron atom—and whose amine function can be differently substituted (different R_1 and R_2, Fig. 2b) to produce hydrophobic and hydrophilic spin-traps (e.g., diethyldithiocarbamate (DETC) and *N*-methyl-D-glucamine dithiocarbamate (MGD), respectively; Fig. 2b). Biding of NO to a ferrous-*bis*-dithiocarbamate ($Fe^{2+}\text{-}(TC)_2$) results in formation of a mononitrosyl-iron complex (MNIC) (Fig. 2c; Eq. 6), that gives rise to a simple EPR signal that can be easily detected and analyzed at room temperature. The formation of MNIC is very fast ($k \approx 10^6$–$10^8\ M^{-1}s^{-1}$ [46–51]) and its stability is high (NO does not dissociate) as long as a high ratio of dithiocarbamate:iron is used (≥10) [51].

$$Fe^{2+}\ (TC)_2 + {}^{\cdot}NO \rightarrow Fe^{2+}\ (TC)_2\ \ NO(\{FeNO\}^7, \text{paramagnetic}) \qquad (6)$$

(*The charge distribution in metal-NO adducts is frequently ambiguous; as such, the Enemark and Feltham notation was adopted,*

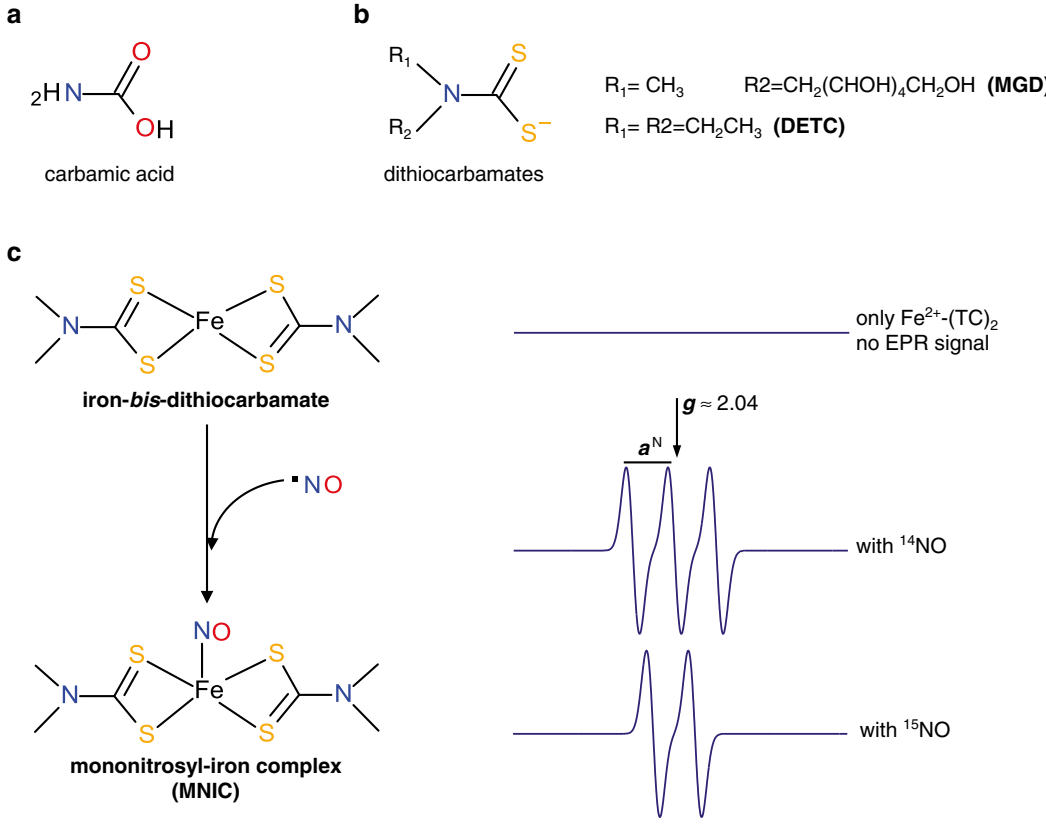

Fig. 2 Iron-dithiocarbamates. (**a**) Structure of the carbamic acid. (**b**) General structure of dithiocarbamates; amine substitutions (R_1 and R_2) of MGD and DETC are shown. (**c**) Structures of $Fe\text{-}(TC)_2$ and $Fe\text{-}(TC)_2$-NO and the respective characteristic EPR spectra $Fe\text{-}(TC)_2$ do not give rise to any EPR signal, while $Fe\text{-}(TC)_2$-^{14}NO and $Fe\text{-}(TC)_2$-^{15}NO yield a triplet and doublet signal, respectively)

{FeNO}n, where the superscript "n" indicates the number of metal d electrons plus the number of NO π-antibonding electrons [52].)

The MNIC EPR signal, with a g value of ≈2.04, is characterized by a 1:1:1 triplet pattern produced by the bound nitrogen atom of *natural* NO ($I(^{14}N) = 1$), with a nitrogen hyperfine splitting constant, a^N, of 1.2–1.3 mT. In the presence of isotopically labeled ^{15}NO, the resulting MNIC will give rise to the doublet signal characteristic of a nucleus with a I of $1/2$, thus, allowing the clear identification of the NO source (e.g., study of NO generation in the presence of NO synthase and L-(^{15}N)-arginine).

The Fe-$(TC)_2$ have been widely used in in vitro studies, with purified and partially purified components [53–61], in vivo and in situ studies, with living animals, tissues, and cells [39–45, 62–70], using hydrophobic (e.g., DETC) and hydrophilic (e.g., MGD) spin-traps to target hydrophilic and lipophylic systems present in "aqueous compartments" and in membranes, respectively.

The Fe-$(TC)_2$ and the respective MNIC are, however, redox active species and care must be taken for possible artifacts. In aqueous solution, the Fe^{2+}-$(TC)_2$ are easily oxidized by dissolved dioxygen ($k \approx 10^5$–10^6 $M^{-1}s^{-1}$ [71, 72]) to the respective ferric complexes (Fe^{3+}-$(TC)_2$), thus, decreasing the concentration of ferrous complex available to detect NO. In addition, and more important, the Fe^{3+}-$(TC)_2$ formed rapidly consumes the NO (Eqs. 7–10; $k \approx 10^8$ $M^{-1}s^{-1}$ for Eq. 7 [46, 49–51]), but to yield an EPR signal whose intensity is less than 50 % of the one that would be originated by the ferrous complex (Eq. 11 vs. Eq. 6) [46, 51, 73–75]:

$$Fe^{3+} - (TC)_2 + {}^{\bullet}NO \rightarrow Fe^{3+} - (TC)_2 - NO(\{FeNO\}^6, \text{diamagnetic}) \quad (7)$$

$$Fe^{3+} - (TC)_2 - NO \rightleftharpoons Fe^{2+} - (TC)_2 - NO^+ (\{FeNO\}^6, \text{diamagnetic}) \quad ((8))$$

$$Fe^{2+} - (TC)_2 - NO^+ \_\_\_ (H_2O \text{ or } HO^-) \rightarrow Fe^{2+} - (TC)_2 + NO_2^- \quad (9)$$

$$Fe^{3+} - (TC)_2 - NO + Fe^{2+} - (TC)_2 \rightarrow Fe^{3+} - (TC)_2 + Fe^{2+} - (TC)_2 - NO\,(\{FeNO\}^7, \text{paramagnetic}) \quad (10)$$

Global reaction (Eqs. 7 + 8 + 9 + 10):

$$Fe^{3+} - (TC)_2 + 2^{\bullet}NO \rightarrow 1Fe^{2+} \quad (TC)_2 - NO(\{FeNO\}^7, \text{paramagnetic}) + NO_2^- \quad (11)$$

In this context, it should be here emphasized that Fe-$(TC)_2$ behaves differently in aqueous and organic solutions (e.g., the hydrophobic DETC–MNIC is not easily oxidized by oxygen and the diamagnetic complex is rapidly converted into the paramagnetic one in a hydrophobic medium [76]).

Fortunately, the oxidation of Fe^{2+}-$(TC)_2$ is easily detected by UV–visible absorption (even at naked eye), as the colorless ferrous complex solution is converted into an orange-brown solution

(details in the Subheading 3) [51, 75]. The potential formation of Fe^{3+}-$(TC)_2$ can also be monitored by EPR at 77 K, following the $g \approx 4.3$ signal characteristic of high-spin Fe^{3+} ($S = 5/2$) [51, 74].

In a similar way, oxidation of Fe^{2+}-$(TC)_2$-NO and Fe^{2+}-$(TC)_2$ by oxidants present in the sample to be analyzed would falsely lead to a decreased EPR signal and, consequently, to an underestimation of the NO present. Yet, the *other side of the coin* is that reducers present in the sample (like ascorbate [51, 72, 77], GSH and L-cysteine [72, 78]) can promote the reduction of Fe^{3+}-$(TC)_2$-NO to the paramagnetic species. Hence, the ratio between reduced and oxidized Fe-$(TC)_2$ and Fe-$(TC)_2$-NO (particularly in cells, tissues and living organisms) would depend on the presence of endogenous and exogenous oxidants and reducers and on the presence of endogenous or exogenous superoxide dismutase and catalase (discussed below).

To sum up, the redox properties of the Fe-$(TC)_2$ and respective MNIC could greatly complicate the quantitative analysis of NO concentration. Accordingly, when possible and reasonable, care must be taken to ensure anaerobic and reducing conditions that preserve the Fe-$(TC)_2$ and Fe-$(TC)_2$-NO complexes in the ferrous state. This would not be possible, or even advisable, in many biological systems or in in vivo and in situ assays. Nevertheless, and most important, a qualitative or comparative analysis could still be made, since Fe^{3+}-$(TC)_2$ would also lead to the formation of measurable paramagnetic MNIC.

Other concern relates to the specificity of the Fe-$(TC)_2$ complexes for NO. There is some controversy regarding their ability to originate paramagnetic complexes with the nitrosonium cation (NO^+) donor sodium nitroprusside and with the nitroxyl anion (NO^-) donor Angeli's salt. The complex resultant from the reaction of Fe^{2+}-$(TC)_2$ with nitroxyl would be EPR silent ($\{FeNO\}^8$) [79], and, while Xia and Zweier [54] in fact did not observed any EPR signal in the presence of Angeli's salt, Komarov et al. [80] did obtain a signal. However, as Xia et al. [81] suggested, the nitroxyl is probably reacting with the oxidized trap (to yield a $\{FeNO\}^7$), which, by intramolecular iron reduction, would result in the expected paramagnetic Fe^{2+}-$(TC)_2$-NO. In its turn, the paramagnetic complex responsible for the nitrosonium signal in the presence of Fe^{2+}-$(TC)_2$ (an initial $\{FeNO\}^6$ complex) [80] could be formed in a similar way to the one suggested for the signal obtained with NO and Fe^{3+}-$(TC)_2$ (also an initial $\{FeNO\}^6$ complex that eventually yields an $\{FeNO\}^7$ species (Eqs. 7–10)). In addition, also S-nitrosoglutathione (GSNO) was shown to elicit the formation of paramagnetic MNIC [78]. In contrast, there is no debate concerning the inability of Fe-$(TC)_2$ to yield EPR signals with nitrite [56, 58–61, 80]. Furthermore, although nitrite was described to be able to oxidize Fe^{2+}-$(TC)_2$, the reaction is too slow to be of any practical relevance ($\approx 5\ M^{-2}s^{-1}$) [75].

Other issues can be raised regarding reactive oxygen species (superoxide radical anion, hydrogen peroxide, hydroxyl radical). Although they can be "normal" products of the system under study, reactive oxygen species can also arise as "by-products" of the dioxygen oxidation of Fe-$(TC)_2$ and, thus, introduce "extra" oxidative damages to the biomolecules ("extra" oxidative stress) or cause artificial NO generation from nitrogenous compounds [71, 78]. Moreover, hydrogen peroxide [72], superoxide and peroxynitrite [48, 77] are able to convert paramagnetic MNIC into EPR silent complexes. Although the reaction of NO with superoxide (to yield peroxynitrite) is considerably faster ($k \approx 7 \times 10^9 M^{-1}s^{-1}$ [12, 13]) than its reaction with Fe-$(TC)_2$, the presence of millimolar Fe-$(TC)_2$ (comparatively to the low (micromolar at most) superoxide concentration normally found) would guarantee the formation of (at least some) Fe-$(TC)_2$-NO. However, the formed Fe^{2+}-$(TC)_2$-NO, present at low concentration, cannot escape to the "attack" of superoxide ($k \approx 3 \times 10^7 M^{-1}s^{-1}$ [77]). In this context, the presence of exogenous and endogenous superoxide dismutase and catalase has to be carefully thought when quantitative analyses of NO concentration are made.

Finally, it should not be overlooked that the Fe-$(TC)_2$ and Fe-$(TC)_2$-NO complexes can also interfere directly with the system under study by inhibiting or inactivating enzymes, receptors, and many other biomolecules. Appropriate controls should be done to guarantee that, e.g., the absence (or weak) of EPR signal is not due to inhibition of the NO generating system; or the opposite, that an intense EPR signal is not the result of the inactivation of the NO target or scavenger. In this respect, particular attention has to be paid to in vivo and in situ studies (where the complexity of the system is very high) and to the use of different Fe-$(TC)_2$ spin-traps, since different substitutions (R_1 and R_2, Fig. 2b) could have dissimilar effects on the biomolecules and be differently accumulated subcellularly. The chelating activity of dithiocarbamates should never be disregarded. Dithiocarbamates are powerful chelators that can chelate free metal ions as well as metal ions present in biomolecules and, in this way, inactivate those biomolecules (e.g., the Cu, Zn-superoxide dismutase inhibition by DETC was attributed to the removal of the enzyme essential copper atom [82]). On the other hand, also the addition of iron can be detrimental (at least through the catalysis of radical species formation).

To conclude, the use each type of spin-trap has its advantages and disadvantages. In this chapter, particular attention was given to Fe-$(TC)_2$ that are the NO traps of choice for the authors. Certainly, the redox chemistry and nature of Fe-$(TC)_2$ and Fe-$(TC)_2$-NO can introduce artifacts and drawbacks in their utilization (Fig. 3). Nonetheless, the careful planning of the assays allows one to avoid the *problems* and use the Fe-$(TC)_2$ as a valuable approach to obtain accurate and reproducible results that cannot be easily acquired other means.

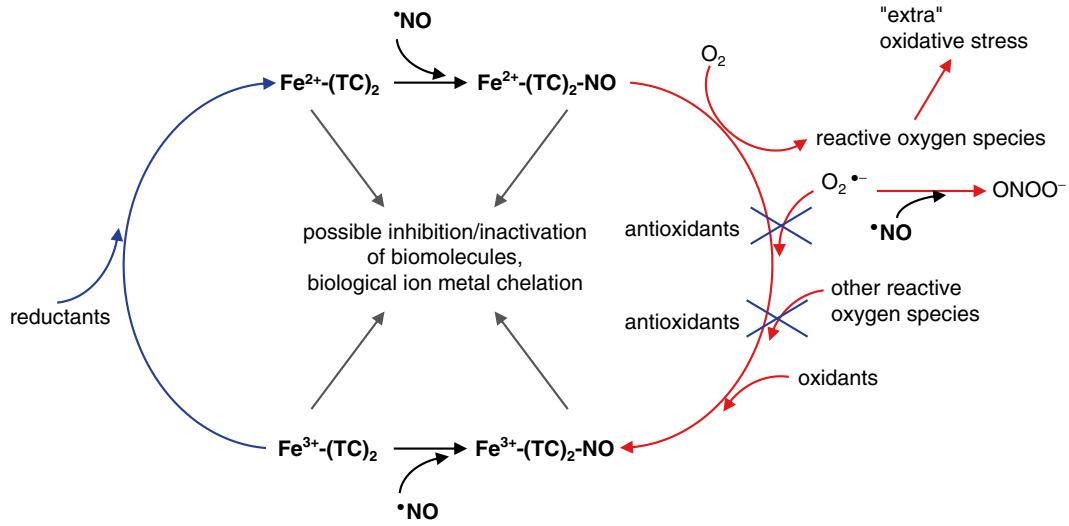

Fig. 3 Possible artifacts introduced by the redox chemistry and nature of Fe-$(TC)_2$ and Fe-$(TC)_2$-NO complexes

1.3 Spin-Trapping with Iron-Dithiocarbamates

The NO spin-trapping with iron-dithiocarbamates methodology is here exemplified using the ability of mammalian xanthine oxidase (XO) and bacterial aldehyde oxidoreductase (AOR) to reduce nitrite to generate NO [60, 61]. The objective is to demonstrate and quantify the NO formation. For that purpose, the protocol is very simple to perform: it involves mixing the enzyme, a reducing substrate and nitrite in the presence of the spin-trap, in a buffered system. The EPR spectrum is, then, acquired. The observation of a triplet signal with the characteristic parameters confirms the presence of NO. The quantification is made with a standard curve prepared with NO solutions of known concentration or by calibration with a nitroxide radical of known concentration. The NO formation over time can be followed through the increase of the signal intensity.

2 Materials

2.1 Preparation of Solutions and Materials for EPR Measurements

Preferably, use in all solutions water first distilled and then deionized (with ≤18 MΩ (25 °C)), to avoid adding unwanted redox active metal ions and other compounds that may interfere with the redox chemistry of the spin-trap and with your system (many enzymes are inhibited by heavy metal ions).

1. MGD (also named *N*-(dithiocarboxy)-*N*-methyl-D-glucamine), sodium salt, with a purity ≥98.0 % (for EPR spectroscopy).
2. Ferrous ammonium sulfate, with a high purity (99.997 %).
3. NO gas, ≈100 % or any percentage prepared by the gases supplier, e.g., 5 % NO/95 % He.

4. Gaseous argon or nitrogen with high purity (>99.999 %).
5. Proper tube to delivery the gases (*see* Fig. 4a, b), which should not be permeable to argon, nitrogen, NO, and oxygen and other gases from the atmosphere.
6. Flasks with a neck suitable to be closed by a rubber stopper and the respective rubber stoppers; aluminum crimp caps (to fix the rubber stoppers, if needed) and a hand-operated aluminum cap crimper.
7. Needles; we find the ones with 0.9×90 mm and 0.8×50 mm suitable to bubble the gas and to act as "escape," respectively (dimensions are diameter×length).
8. *Gastight* syringes.
9. Flat cell or 50 μL capillaries.
10. X-band (9.5 GHz) EPR spectrometer.

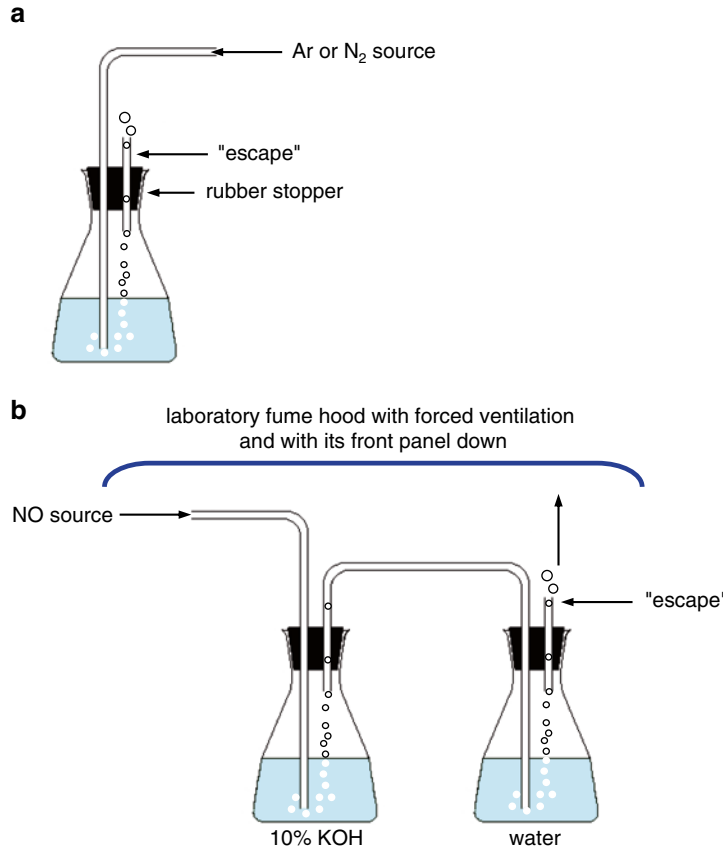

Fig. 4 Settings used to prepare deoxygenated solutions (**a**) and the stock NO saturated solution (**b**)

2.2 For the AOR and XO-Dependent NO Generation Assays

1. Buffer: 50 mM phosphate buffer, pH 6.0–7.8, 100 mM MES buffer for pH 5.5–6.0; 100 mM Tris–HCl buffer is also suitable for pH 7–9.
2. The enzymes used are purified, but partially purified samples or crude extracts can also be used.
3. Nitrite.
4. Reducing substrate, xanthine for the XO reaction and benzaldehyde for the AOR reaction (*see* **Note 1**).

3 Methods

As described in the "Introduction," if the system and study aims allow it, take great care to guarantee anaerobic (deoxygenated) conditions throughout all the procedure (*see* **Note 2**). In this way, the Fe-$(MGD)_2$ and Fe-$(MGD)_2$-NO complexes would be maintained in the ferrous state (*see* **Note 3**). The anaerobic conditions can be achieved by using flasks sealed with rubber stoppers and purging the solutions or water with an inert gas, nitrogen, or argon (*see* **Note 4**) (Fig. 4a). Also the MGD and iron powders have to be deoxygenated in sealed flaks before the addition of the solution in which they will be dissolved. To transfer the solutions/water from one flask to another or to the EPR flat cell, use *gastight* syringes (syringes whose plunger tip, often in PTFE, creates a leak-free seal, e.g., Hamilton® GASTIGHT® Syringes). During the transfer operations, be very careful to avoid contaminations by oxygen from the atmosphere. Ideally, the assay mixtures should be prepared inside an anaerobic chamber (*see* **Note 5**), as this allows one to manipulate the solutions and powders without taking the risk of contaminating them with the atmospheric oxygen.

3.1 Preparation of Fe-$(MGD)_2$

1. The two solids, MGD and ferrous ammonium sulfate, should be brought together and deoxygenated in a sealed flask; subsequently, deoxygenated buffer or water should be added to dissolve them.
2. Prepare the solution only immediately before use—do not use "old" solutions.
3. Weight the necessary masses to prepare a mixture of 20 mM MGD:2 mM iron, final concentrations.
4. A high MGD:iron ratio is important to ensure the stability of the future Fe^{2+}-$(MGD)_2$-NO complex (*see* **Note 6**).
5. However after a first trial, you may want to test a lower ratio to save MGD. In our assays, we use a ratio of 10 (5 mM MGD:0.5 mM iron) with the DEAE NO donor, while a ratio of 5 (10 mM MGD:2 mM iron, final concentrations) results very well with purified enzymes [60, 61].

The Fe^{2+}-$(MGD)_2$ solution should be light colorless and the potential formation of ferric complexes can be easily followed and quantified through the UV–visible spectrum due to their orange-brown coloration [maximum absorption at 340 nm ($\varepsilon = 20{,}000\ M^{-1}\ cm^{-1}$) and shoulders at 385 nm ($\varepsilon = 15.000\ M^{-1}\ cm^{-1}$) and 520 nm ($\varepsilon = 3.000\ M^{-1}\ cm^{-1}$).

3.2 Preparation of Stock NO Saturated Solution

1. The saturated solution of NO is prepared by bubbling NO gas, first, in a potassium hydroxide 10 % solution, to remove other nitrogen oxides present in the NO gas, and, then, in water, as shown in Fig. 4b (*see* **Notes 7** and **8**).
2. It is crucial that the potassium hydroxide solution is prepared in deoxygenated, deionized water, and the "final" water (where NO gas will be dissolved) should also be deoxygenated and deionized (follow the indications provided in the beginning of this section on how to deoxygenate solutions).
3. The NO purging should be performed in an ice-water bath, because lower temperatures increase the NO solubility in solution (*see* **Note 9**). The NO bubbling time is dependent on the NO gas concentration: for a pure gas (≈100 % NO), 10 min would be sufficient, but, for a 5 % gas (5 % NO/95 % He), purge for at least 30 min.
4. After that time, close the NO source and, immediately, remove the two needles from the water flask (*see* **Note 10**).
5. The concentration of NO dissolved in water is dependent on the percentage of NO gas used and on the temperature: for ≈100 % NO, it is ≈3.3 and ≈1.91 mM, at 0 and 20 °C, respectively, and for 5 % NO, it is ≈170 and ≈100 μM, at 0 and 20 °C, respectively. Dilutions can be, then, prepared from the stock NO saturated solution (*see* **Note 11**).

3.3 Preparation of Reaction Mixtures

1. Deoxygenate all solutions immediately before being used.
2. Prepare your reactions mixtures starting with the buffer and spin-trap; the NO generating/consuming system should be the last to be added (this is the moment that establishes the "time zero" of the reaction and the spin-trap must already be present to trap the NO).
3. For the AOR- and XO-catalyzed nitrite-dependent NO generation, this means that the additions should be made by the following order: buffer (and water if necessary), spin-trap, enzyme, reducing substrate and at least nitrite.
4. Usually, the measurements are carried out in 275–300 μL flat cells (*see* **Note 12**), but 50 μL capillaries can also be used to save sample, if it has a sufficiently high concentration of paramagnetic species to give rise to a measurable signal with the smaller sample amount.

5. If an anaerobic chamber is used to prepare the reactions mixtures, filling the flat cell or the capillary should be an easy task, using a simple glass pipette, or by capillarity, respectively (both ends of the capillary should then be sealed).
6. But, if an anaerobic chamber is not available, it would be very difficult to work with capillaries and maintain the anaerobic conditions.
7. Regarding the flat cell, this must be first sealed with a rubber stopper and made anaerobic; after that, the sample can be transferred with a *gastight* syringe.

3.4 EPR Measurements

1. The EPR signal of the Fe^{2+}-$(MGD)_2$-NO complex has a g value of ≈2.04, an a^N of 1.2–1.3 mT and an 1:1:1 triplet or 1:1 doublet pattern, depending if it is originated from ^{14}NO or isotopically labeled.
2. In an X-band EPR spectrophotometer, with a frequency of 9.7 GHz, the signal will be centered around 340 mT (Eq. 2b) and a window width of 8 mT would be ample to display the signal.
3. A modulation amplitude of 0.1–0.3 mT is used and the microwave power needed would depend on the concentration of paramagnetic complexes present; usually a value between 10 and 100 mW is employed (*see* **Note 13**).
4. The observation of the characteristic signal confirms the presence of NO in the sample.
5. For the AOR and XO assays, the use of *normal* nitrite (that is, with naturally abundant isotope of nitrogen (^{14}N)) and of isotopically labeled $^{15}NO_2^-$, results in the expected triplet and doublet signals, respectively. These two results demonstrate that is nitrite the source of NO.
6. To quantify the concentration of NO (or more precisely of Fe^{2+}-$(MGD)_2$-NO), a standard curve can be prepared using the spin-trap and solutions equilibrated with different NO concentrations prepared from the stock NO saturated solution.
7. It is crucial, that the standard curve is obtained under the same conditions as the assays, same buffer composition (buffer species and other compounds present, concentration, pH, and ionic strength), temperature, and spin-trap concentration.
8. The EPR signal is exactly the same in both cases, the signal intensity of the assay and standard can be measured by the height of one of its three lines, or by the double integral (*see* **Note 14**)—what is easier for the researcher.
9. Quantification can also be performed by comparison with the signal of 2,2,6,6-tetramethylpiperidinyl-*N*-oxyl (TEMPO). TEMPO is a nitroxide radical that gives rise to a triplet signal,

with an a^N of ≈1.75 mT, and the double integral of its signal provides a relation area—concentration that can be subsequently used to convert the areas of the signal of the assays into concentration values (*see* **Note 15**).

10. In general, Fe^{2+}-$(MGD)_2$-NO as low as 10 nM can be detected, with the advantage that also kinetics of NO increase can be easily followed in one unique sample.
11. Because of the high stability of the Fe^{2+}-$(MGD)_2$-NO complex, NO decreases over time could not be measured in the only one sample.
12. Yet, different samples can be prepared to be read at different times.
13. For the AOR and XO assays, the concentration of NO formed is dependent on the reducing substrate and nitrite concentration, on the pH and also on the enzyme concentration/time of reaction.
14. Different proportions of reducing substrate/nitrite should be assayed to find the ones that give rise to better results at each pH value.

3.5 Controls

As in other methodologies, it is essential to carry out the appropriate controls to guarantee that the conclusions drawn are correctly supported.

The first obligate controls involve the study of the potential Fe^{2+}-$(MGD)_2$-NO formation in the absence of each individual component of the system. For the AOR- and XO-catalyzed nitrite-dependent NO generation, the Fe^{2+}-$(MGD)_2$-NO formation should be studied in the absence of nitrite (presence of all the other components), absence of enzyme (presence of all the other components), and absence of reducing substrate (presence of all the other components). No observation of EPR signal in the absence of any of the three components demonstrates that it is the enzyme (AOR or XO) that is responsible for the NO formation. The observation of EPR signal in the presence of reducing substrates of different nature further confirms the XO ability to form NO (*see* **Note 16**). To discriminate if it is an enzymatic reaction, or, on the contrary, is just a nonspecific reaction carried out by the protein moiety, test the inactivated or denaturated enzyme.

If no EPR signal is observed in a situation where it is expected the NO formation, investigate the interference of Fe^{2+}-$(MGD)_2$ and Fe^{2+}-$(MGD)_2$-NO with the system, for example, the potential enzyme inhibition.

Another control that can be helpful in case of no EPR signal formation is to test if the *medium/conditions* of the system interfere with the Fe^{2+}-$(MGD)_2$-NO formation. For this, test the ability of Fe^{2+}-$(MGD)_2$ to generate the paramagnetic species with the stock NO saturated solution under the same *medium/conditions* used in the system under study. If, hypothetically, the buffer hinders the formation of the Fe^{2+}-$(MGD)_2$-NO complex, then no

EPR signal will be formed either with the stock NO solution or with your system.

Pay special attention to the controls, if you use partially purified enzymes or crude extracts, as the number of problems that can arise are proportional to the complexity of the system under study.

4 Notes

1. The reducing substrate reacts with the enzyme; the reduced enzyme, then, reduces nitrite to NO, closing the catalytic cycle. Other reducing substrates of each enzyme can be equally employed.
2. However, even if the Fe^{2+}-$(MGD)_2$ solution is mostly oxidized to the ferric state, the formation of measurable paramagnetic Fe^{2+}-$(MGD)_2$-NO may not be hindered (via Eq. 11 and through reducing compounds present in the sample that can reduce the ferric complexes back to Fe^{2+}-$(MGD)_2$ and Fe^{2+}-$(MGD)_2$-NO). The possible presence of antioxidants, as well as, of oxidants must be considered.
3. Note that the preparation of Fe-$(MGD)_2$ under aerobic conditions leads to its rapid and uncontrolled oxidation to Fe^{3+}-$(MGD)_2$ prior to its utilization. Moreover, after addition to the system, the concomitantly reduced oxygen would scavenge the NO and increase the oxidative stress induced in the system. These should affect (diminish) the reproducibility and accuracy of the data to be obtained. Therefore, even if the assays are to be performed under aerobic conditions, prepare the spin-trap under anaerobic conditions and tightly control the timing when it becomes in contact with oxygen.
4. To deoxygenate a solution/water (or a powder), the dissolved oxygen must be removed, being replaced by an inert gas, nitrogen, or argon. To do this, bubble the inert gas into the solution/water (it can be done under stirring to facilitate the gases exchange). For oxygen to be released (and do not build in pressure), a pressure relief must be provided during purging (an "escape"), which is usually achieved by the insertion of a second needle that must not touch the liquid, as illustrated in Fig. 4a. The bubbling time should be proportional to the volume of liquid to be deoxygenated; for 10–20 mL, 30 min would be sufficient. The efficiency of deoxygenation can be greatly improved if purging is intercalated by an equal time period of vacuum (usually three cycles of purging/vacuum are sufficient). Regarding the choice of the inert gas: argon is more expensive than nitrogen, but, because it is heavier, its "deoxygenation ability" is more efficient. Obviously, this procedure also removes carbon dioxide and other atmospheric gases that are dissolved in the solutions/water.

5. Please refer to the instructions of the respective anaerobic chamber (also known as glove box) before attempting to use it. Although all solutions and powders must be made anaerobic before entering the anaerobic chamber (that is, that part cannot be circumvented), the use of an anaerobic chamber avoids the problems of oxygen contaminations during the transfer and mixing procedures.
6. In in vivo or in situ assays, guarantee that MGD and iron are added in sufficient concentration to facilitate the formation of a high MGD:iron ration inside the cells; also consider the solubility of the trap chosen (MGD and DETC accumulate in aqueous and lipidic compartments).
7. The NO gas handling must be performed only in a laboratory fume hood with forced ventilation and with its front panel down. The personnel handling the gas must be thoroughly familiar with the Material Safety Data Sheet and with the proper handling procedures.
8. With the setting shown in Fig. 4b, be particularly cautious, because the gas "escape" is present only in the water flask. You must confirm that NO is bubbling through the KOH solution to the "final" water flask, not only for safety reasons, but also to guarantee that the water is in fact being saturated with NO.
9. At room temperature, the NO solubility would decrease, but, in this way, when you use the solution at room temperature you will be sure that the solution is truly saturated with NO.
10. If the two needles are not removed immediately, the oxygen from the atmosphere will get in into the solution through the "escape" needle and the NO concentration will be decreased (NO reacts with oxygen to yield nitrogen dioxide radical and other products).
11. When working outside an anaerobic chamber, do not forget to be very careful during the dilutions to avoid contamination with the oxygen from the atmosphere.
12. The common 4 mm (internal diameter) tube cannot be used in X-band EPR spectroscopy at room temperature of aqueous solutions, because the water present in the sample hinders the measurements: the electric dipole moment of the water molecule interacts with the electric field in the resonator and a large amount of the microwave energy is absorbed (lost) by the water. To circumvent the problem created by liquids with dielectric loss (in X-band EPR cavities) one can use flat cells, which confine the sample to a 0.3 mm thick space, in a volume typically of 275–300 μL. The flat cell has to be placed in the rectangular cavity exactly perpendicularly to the external magnets, parallel to the electric field, in a nodal plane where the electric field intensity is minimal and the magnetic field is maxi-

mal; a few degrees of misalignment of the cell inside the cavity results in a sharp increase in the dissipated (lost) energy, with the concomitant decrease in the energy stored to drive the absorption by EPR. Alternatively, a 50 μL capillary, with an internal diameter of 0.8 mm, can solve the problem if the sample has a sufficiently high concentration of paramagnetic species to give rise to a measurable signal with the small sample amount.

13. Confirm that your signal is not saturated. For a nonsaturated signal, the intensity is directly proportional to the square root of the power. The intensity can be determined by measuring the height of one of the signal three lines, or by the double integral (*see also* **Note 14**).
14. Note that it is necessary to calculate the double integral, because the EPR spectrum is recorded as the first derivative of absorption (double integral = area under the absorption line).
15. The direct comparison of EPR spectra is possible, because the intensity of an EPR signal is independent of the species that has originated it (it is not necessary the previous knowledge of an extinction coefficient). The use of TEMPO or NO saturated solution may depend on their availability. The usage of a NO saturated solution has the advantage of providing hints of possible problems arising from the assay system/mixture, if it is possible to compare the results obtained in different media.
16. It is known that XO displays catalytic activity (oxygen-reducing activity) with reducing substrates of different nature (e.g., purines and aldehydes), being classified as a promiscuous enzyme.

Acknowledgments

This work was supported by the Unidade de Ciências Biomoleculares Aplicadas-UCIBIO which is financed by national funds from FCT/MEC (UID/Multi/04378/2013) and co-financed by the ERDF under the PT2020 Partnership Agreement (POCI-01-0145-FEDER-007728.

References

1. Moncada S, Palmer RMJ, Higgs EA (1991) Nitric oxide: physiology, pathophysiology, and pharmacology. Pharmacol Rev 43:109–142
2. Gusarov I, Nudler E (2005) NO-mediated cytoprotection: instant adaptation to oxidative stress in bacteria. Proc Natl Acad Sci U S A 102:13855–13860
3. Neill S, Bright J, Desikan R, Hancock J, Harrison J, Wilson I (2008) Nitric oxide evolution and perception. J Exp Bot 59:25–35
4. Wilson ID, Neill SJ, Hancock JT (2008) Nitric oxide synthesis and signalling in plants. Plant Cell Environ 31:622–631
5. Gupta KJ, Kaiser WM (2010) Production and scavenging of nitric oxide by barley root mitochondria. Plant Cell Physiol 51:576–584
6. Moreau M, Lindermayr C, Durner J, Klessig DF (2010) NO synthesis and signaling in plants -where do we stand? Physiol Plant 138: 372–383

7. Toledo JC, Augusto O (2012) Connecting the chemical and biological properties of nitric oxide. Chem Res Toxicol 25:975–989
8. Maia L, Moura JJG (2014) How biology handles nitrite. Chem Rev 114:5273–5357
9. Dalton LR (ed) (1985) EPR and advanced EPR studies of biological systems. CRC Press, Boca Raton
10. Palmer G (1985) The electron paramagnetic resonance of metalloproteins. Biochem Soc Trans 13:548–560
11. Weil JA, Bolton JR, Wertz JE (1994) Electron paramagnetic resonance: elementary theory and practical applications. Wiley, New York
12. Beckman JS, Koppenol WH (1996) Nitric oxide, superoxide and peroxynitrite: the good, the bad and the ugly. Am J Physiol 271:C1424–C1437
13. Koppenol WH (1998) The basic chemistry of nitrogen monoxide and peroxynitrite. Free Radic Biol Med 25:385–391
14. Wink DA, Mitchell JB (1998) Chemical biology of nitric oxide: insights into regulatory, cytotoxic, and cytoprotective mechanisms of nitric oxide. Free Radic Biol Med 25:434–456
15. Feelisch M, Rassaf T, Mnaimneh S, Singh N, Bryan NS, Jourd'Heuil D, Kelm M (2002) Concomitant S-, N-, and heme-nitros(yl) ation in biological tissues and fluids: implications for the fate of NO in vivo. FASEB J 16: 1775–1785
16. Taha ZH (2003) Nitric oxide measurements in biological samples. Talanta 61:3–10
17. Bryan NS, Rassaf T, Maloney RE, Rodriguez CM, Saijo F, Rodriguez JR, Feelisch M (2004) Cellular targets and mechanisms of nitros(yl) ation: an insight into their nature and kinetics in vivo. Proc Natl Acad Sci U S A 101: 4308–4313
18. Perkins MJ (1980) Spin trapping. Adv Phys Org Chem 17:1–64
19. Janzen EG, Haire DL (1990) Two decades of spin trapping. Adv Free Rad Chem 1:253–295
20. Davies MJ, Timmins GS, Clark RJH, Hester RE (1996) EPR spectroscopy of biologically relevant free radicals in cellular, ex vivo, and in vivo systems. In: Clark RJH, Hester RE (eds) Biomedical applications of spectroscopy. John Wiley & Sons, New York
21. Berliner LJ, Khramtsov V, Fujii H, Clanton TL (2001) Unique in vivo applications of spin traps. Free Radic Biol Med 30:489–499
22. Villamena FA, Zweier JL (2004) Detection of reactive oxygen and nitrogen species by EPR spin trapping. Antioxid Redox Signal 6:619–629
23. Davies MJ (1993) Detection and identification of macromolecule-derived radicals by EPR spin trapping. Res Chem Intermed 19:669–679
24. Clement JL, Gilbert BC, Rockenbauer A, Tordo P (2001) Radical damage to proteins studied by EPR spin-trapping techniques. J Chem Soc Perkin Trans 2:1463–1470
25. Davies MJ, Hawkins CL (2004) EPR spin trapping of protein radicals. Free Radic Biol Med 36:1072–1086
26. Akaike T, Yoshida M, Miyamoto Y, Sato K, Kohno M, Sasamoto K, Miyazaki K, Ueda S, Maeda H (1993) Antagonistic action of imidazolineoxyl N-oxides against endothelium-derived relaxing factor/.bul.NO (nitric oxide) through a radical reaction. Biochemistry 32:827–832
27. Joseph J, Kalyanaraman B, Hyde JS (1993) Trapping of nitric oxide by nitronyl nitroxides: an electron spin resonance investigation. Biochem Biophys Res Commun 192:926–934
28. Hogg N, Singh RJ, Joseph J, Neese F, Kalyanaraman B (1995) Reactions of nitric oxide with nitronyl nitroxides and oxygen: prediction of nitrite and nitrate formation by kinetic simulation. Free Radic Res 22:47–56
29. Grätzel M, Taniguchi S, Henglein Ber A (1970) Pulsradiolytische Untersuchung der NO-Oxydation und des Gleichgewichts $N_2O_3 \rightarrow NO + NO_2$ in wäßriger Lösung. Ber Bunsen-Ges Phys Chem 74:488–492
30. Treinin A, Hayon E (1970) Absorption spectra and reaction kinetics of NO_2, N_2O_3, and N_2O_4 in aqueous solution. J Am Chem Soc 92:5821–5828
31. Singh RJ, Hogg N, Joseph J, Konorev E, Kalyanaraman B (1999) The peroxynitrite generator, SIN-1, becomes a nitric oxide donor in the presence of electron acceptors. Arch Biochem Biophys 361:331–339
32. Zhang Y, Hogg N (2004) Formation and stability of S-nitrosothiols in RAW 2647 cells. Am J Physiol Lung Cell Mol Physiol 287: L467–L474
33. Zhang Y, Hogg N (2002) Mixing artifacts from the bolus addition of nitric oxide to oxymyoglobin: implications for s-nitrosothiol formation. Free Radic Biol Med 32:1212–1219
34. Piknova B, Gladwin MT, Schechter AN, Hogg N (2005) Electron paramagnetic resonance analysis of nitrosylhemoglobin in humans during NO inhalation. J Biol Chem 280:40583–40588
35. Hille R, Olson JS, Palmer G (1979) Spectral transitions of nitrosyl hemes during ligand binding to hemoglobin. J Biol Chem 254:12110–12120
36. Louro SR, Ribeiro PC, Bemski G (1981) EPR spectral changes of nitrosyl hemes and their relation to the hemoglobin T-R transition. Biochim Biophys Acta 670:56–63
37. Kozlov AV, Staniek K, Nohl H (1999) Nitrite reductase activity is a novel function of mammalian mitochondria. FEBS Lett 454: 127–130

38. Huang KT, Keszler A, Patel N, Patel RP, Gladwin MT, Kim-Shapiro DB, Hogg N (2005) The reaction between nitrite and deoxyhemoglobin - reassessment of reaction kinetics and stoichiometry. J Biol Chem 280: 31126–31131
39. Vanin AE, Mordvintcev EI, Kleschyov AL (1984) Biotransformation of sodium nitroprusside into dinitrosyl iron complexes in tissue of ascites tumors of mice. Stud Biophys 102:135–143
40. Varich VJ, Vanin AE, Ovsyannikova LM (1987) Discovery of endogenous nitric oxide in the mouse liver by electron paramagnetic resonance. Biofizika 32:1064–1065
41. Mordvintcev P, Mülsch A, Busse R, Vanin A (1991) On-line detection of nitric oxide formation in liquid aqueous phase by electron paramagnetic resonance spectroscopy. Anal Biochem 199:142–146
42. Kubrina LN, Caldwell WS, Mordvintcev EI, Malenkova IV, Vanin AF (1992) EPR evidence for nitric oxide production from guanidino nitrogen of L-arginine in animal tissues in vivo. Biochim Biophys Acta 1099:233–237
43. Komarov A, Mattson D, Jones MM, Singh PK, Lai CS (1993) In vivo spin trapping of nitric oxide in mice. Biochem Biophys Res Commun 195:1191–1198
44. Komarov AM, Lai CS (1995) Detection of nitric oxide production in mice by spin-trapping electron paramagnetic resonance spectroscopy. Biochim Biophys Acta 1272:29–36
45. Vanin AF, Huisman A, Van Faassen E (2002) Iron dithiocarbamate as spin trap for nitric oxide detection: pitfalls and successes. Methods Enzymol 359:27–42
46. Fujii S, Yoshimura T, Kamada H (1996) Nitric oxide trapping efficiencies of water-soluble iron(III) complexes with dithiocarbamate derivatives. Chem Lett 1996:785–786
47. Paschenko SV, Khramtsov VV, Scatchkov MP, Plyusnin VF, Bassenge E (1996) EPR and laser flash photolis studies of the reaction of nitric oxide with water soluble NO trap Fe(II)-proline-dithiocarbamate complex. Biochem Biophys Res Commun 225:577–584
48. Pou S, Tsai P, Porasuphatana S, Halpern HJ, Chandramouli GV, Barth ED, Rosen GM (1999) Spin trapping of nitric oxide by ferrochelates: kinetic and in vivo pharmacokinetic studies. Biochim Biophys Acta 1427:216–226
49. Fujii S, Kobayashi K, Tagawa S, Yoshimura T (2000) Reaction of nitric oxide with the iron(III) complex of N-(dithiocarboxy)sarcosine: a new type of reductive nitrosylation involving iron(IV) as an intermediate. J Chem Soc Dalton Trans:3310–3315
50. Fujii S, Yoshimura T (2000) A new trend in iron–dithiocarbamate complexes: as an endogenous NO trapping agent. Coord Chem Rev 198:89–99
51. Vanin AF, Liu XP, Samouilov A, Stukan RA, Zweier JL (2000) Redox properties of iron–dithiocarbamates and their nitrosyl derivatives: implications for their use as traps of nitric oxide in biological systems. Biochim Biophys Acta 1474:365–377
52. Enemark JH, Feltham RD (1974) Principles of structure, bonding, and reactivity metal nitrosyl complexes. Coord Chem Rev 13:339–406
53. Miilsch A, Vanin A, Mordvintcev R, Hauschildt S, Busse R (1992) NO accounts completely for the oxygenated nitrogen species generated by enzymic L-arginine oxygenation. Biochem J 288:597–603
54. Xia Y, Zweier JL (1997) Direct measurement of nitric oxide generation from nitric oxide synthase. Proc Natl Acad Sci U S A 94: 12705–12710
55. Yoneyema H, Kosaka H, Ohnishi T, Kawazoe T, Mizoguchi K, Ichikawa Y (1999) Reaction of neuronal nitric oxide synthase with the nitric oxide spin-trapping agent, iron complexed with N-dithiocarboxysarcosine. Eur J Biochem 266:771–777
56. Li H, Samouilov A, Liu X, Zweier JL (2001) Characterization of the magnitude and kinetics of xanthine oxidase catalyzed nitrite reduction: evaluation of its role in nitric oxide generation in anoxic tissues. J Biol Chem 276:24482–24489
57. Huisman A, Vos I, van Faassen EE, Joles JA, Grone HJ, Martasek P, Zonneveld AJ, Vanin AF, Rabelink TJ (2002) Anti-inflammatory effects of tetrahydrobiopterin on early rejection in renal allografts: modulation of inducible nitric oxide synthase. FASEB J 16:1135–1137
58. Li H, Cui H, Kundu TK, Alzawahra W, Zweier JL (2008) Nitric oxide production from nitrite occurs primarily in tissues not in the blood: Critical role of xanthine oxidase and aldehyde oxidase. J Biol Chem 283:17855–17863
59. Li H, Kundu TK, Zweier JL (2009) Characterization of the magnitude and mechanism of aldehyde oxidase-mediated nitric oxide production from nitrite. J Biol Chem 284: 33850–33858
60. Maia L, Moura JJG (2011) Nitrite reduction by xanthine oxidase family enzymes: a new class of nitrite reductases. J Biol Inorg Chem 16:443–460
61. Maia L, Moura JJG (2014) Nitrite reductase activity of rat and human xanthine oxidase, xanthine dehydrogenase, and aldehyde oxidase: evaluation of their contribution to NO formation in vivo. Biochemistry. doi:10.1021/bi500987w
62. Tominaga T, Sato S, Ohnishi T, Ohnishi ST (1993) Potentiation of nitric oxide formation following with bilateral carotid occlusion and

local cerebral ischemia in the rat: in vivo detection of the nitric oxide radical by electron paramagnetic resonance spin trapping. Brain Res 614:342–346
63. Lai CS, Komarov AM (1994) Spin trapping of nitric oxide produced in vivo in septic-shock mice. FEBS Lett 345:120–124
64. Zweier JL, Wang P, Kuppusamy P (1995) Direct measurement of nitric oxide generation in the ischemic heart using electron paramagnetic resonance spectroscopy. J Biol Chem 270:304–307
65. Zweier JL, Wang P, Samouilov A, Kuppusamy P (1995) Enzyme-independent formation of nitric oxide in biological tissues. Nat Med 1:804–809
66. Kuppusamy P, Wang P, Samouilov A, Zweier JL (1996) Spatial mapping of nitric oxide generation in the ischemic heart using electron paramagnetic resonance imaging. Magn Reson Med 36:212–218
67. Yoshimura T, Yokoyama H, Fujii S, Takayama F, Oikawa K, Kamada H (1996) In vivo EPR detection and imaging of endogenous NO in LPS-treated mice. Nat Biotechnol 14:992–994
68. Fujii H, Koscielniak J, Berliner LJ (1997) Determination and characterization of nitric oxide generation in mice in vivo L-band EPR spectroscopy. Magn Res Med 38:565–568
69. Mikoyan VD, Kubrina LN, Serezhenkov VA, Stukan RA, Vanin AF (1997) Complexes of Fe2+ with diethyldithiocarbamate or N-methyl-D-glucamine dithiocarbamate as traps of nitric oxide in animal tissues: comparative investigations. Biochim Biophys Acta 1336:225–234
70. Kotake Y, Moore DR, Sang H, Reinke LA (1999) Continuous monitoring of in vivo nitric oxide formation using EPR analysis in biliary flow. Nitric Oxide 3:114–122
71. Tsuchiya K, Jiang JJ, Yoshizumi M, Tamaki T, Houchi H, Minakuchi K, Fukuzawa K, Mason RP (1999) Nitric oxide-forming reactions of the water-soluble nitric oxide spin-trapping agent, MGD. Free Radic Biol Med 27: 347–355
72. Lu C, Koppenol WH (2005) Redox cycling of iron complexes of N-(dithiocarboxy)sarcosine and N-methyl-d-glucamine dithiocarbamate. Free Radic Biol Med 39:1581–1590
73. Tsuchiya K, Takasugi M, Minakuchi K, Fukuzawa K (1996) Sensitive quantitation of nitric oxide by EPR spectroscopy. Free Radic Biol Med 21:733–737
74. McGrath C, O'Connor C, Sangregodo C, Seddon J, Sinn E, Sowrey E, Young N (1999) Direct measurement of the high-spin and low-spin bond lengths and the spin state population in mixed spin state systems: an Fe K-edge XAFS study of iron(III) dithiocarbamate complexes. Inorg Chem Commun 2:536–539
75. Tsuchiya K, Yoshizumi M, Houchi H, Mason R (2000) Nitric oxide-forming reaction between the iron-N-methyl-D-glucamine dithiocarbamate complex and nitrite. J Biol Chem 275:1551–1556
76. Kubrina LN, Mikoyan VD, Mordvintcev PI, Vanin AF (1993) Iron potentiates lipopolysaccharide-induced nitric oxide formation in animal organs. Biochim Biophys Acta 1176:240–244
77. Vanin AF, Huisman A, Stroes ESG, Ruijter-Heijstek FC, Rabelink TJ, Faassen EE (2001) Antioxidant capacity of mononitrosyl-iron-dithiocarbamate complexes: implications for NO trapping. Free Radic Biol Med 30: 813–824
78. Tsuchihashi K, Kirima K, Yoshizumi M, Houchi H, Tamaki T, Mason RP (2002) The role of thiol and nitrosothiol compounds in the nitric oxide-forming reactions of the iron-N-methyl-D-glucamine dithiocarbamate complex. Biochem J 367:771–779
79. Stamler JS, Singel DJ, Loscalzo J (1992) Biochemistry of nitric oxide and its redox-activated forms. Science 258:1898–1902
80. Komarov AM, Wink DA, Feelisch M, Schmidt HHW (2000) Electron-paramagnetic resonance spectroscopy using N-methyl-D-glucamine dithiocarbamate iron cannot discriminate between nitric oxide and nitroxyl: implications for the detection of reaction products for nitric oxide synthase. Free Radic Biol Med 28:739–742
81. Xia Y, Cardounel AJ, Vanin AF, Zweier JL (2000) Electron paramagnetic resonance spectroscopy with N-methyl-D-glucamine dithiocarbamate iron complexes distinguishes nitric oxide and nitroxyl anion in a redox-dependent manner: applications in identifying nitrogen monoxide products from nitric oxide synthase. Free Radic Biol Med 29:793–797
82. Cocco D, Calabrese L, Rigo A, Agrese E, Rotilio G (1981) Re-examination of the reaction of diethyldithiocarbamate with the copper of superoxide dismutase. J Biol Chem 256:8983–8986